TEMPORAL VARIATIONS IN THE SECOND-DEGREE STOKES TESSERAL GEOPOTENTIAL COEFFICIENTS FROM TOPEX/POSEIDON ALTIMETRY

MILAN BURŠA
Astronomical Institute, Academy of Sciences of the Czech Republic, Prague, CR, E-mail: bursa@ig.cas.cz

STEVE KENYON
National Imagery and Mapping Agency, St.Louis, MO 63118–3399, U.S.A., E-mail: kenyons@nima.mil

JAN KOUBA
Geodetic Survey Division, Natural Resources Canada, Ottawa, Canada, E-mail: kouba@geod.nrcan.gc.ca

ZDISLAV ŠÍMA
Astronomical Institute, Academy of Sciences of the Czech Republic, Prague, CR, E-mail: sima@ig.cas.cz

VILIAM VATRT
Geographical Service of the Czech Armed Forces, Topographical Institute VTOPU, Dobruška, CR, E-mail: vatrt@vghur.army.cz

VOJTĚCH VÍTEK
Lipnická 1219, 39601 Humpolec, Czech Republic

MARIE VOJTÍŠKOVÁ
Geographical Service of the Czech Armed Forces, Topographical Institute VTOPU, Dobruška, CR, E-mail: vojtiskova@vghur.army.cz

(Received 31 March 2003; Accepted 31 December 2003)

Abstract. The TOPEX/POSEIDON (T/P) altimetry data set covering the period of January 1, 1993 to January 3, 2001 was used to derive monthly series of the second-degree tesseral geopotential coefficients. To account for the sea water temperature variations, rather simple models have been devised and discussed, describing localized as well as areal variations of sea water temperature and heights. The second-degree tesseral coefficients have also been shown to be proportional to the pressure portions of the oceanic equatorial effective excitation functions, used in Ocean Angular Momentum (OAM) data. OAM data together with Atmospheric Angular Momentum (AAM) data can be used to study observed polar motion (PM) series. The excess PM rates, derived from the T/P effective excitation functions, were compared to the corresponding observed PM rates, derived from the International Earth Rotation Service (IERS) Bulletin A and corrected with AAM also obtained from IERS. The noise of the T/P derived PM rate series was found to be significantly larger than the corresponding Bulletin A/AAM PM rate residuals as well as the PM rates derived from an independent OAM series that was also available for the 1993–2000 period.

Keywords: T/P altimetry, Stokes 2-nd degree tesseral coefficients–variations, polar motion

Earth, Moon and Planets **93:** 37–64, 2003.

1. Introduction

Because of seasonal variations of the mean ocean level, the Earth's inertia tensor I also varies. The transfer of mass within the ocean–atmosphere bodies and the steric effects give rise to the variations of the inertia tensor elements I_{ik},

$$I_{ik} = \int_M \sum_{j=1}^{3} (\delta_{ik} x_j^2 - x_i x_k)\, \mathrm{d}m; \quad (i, k = 1, 2, 3), \tag{1}$$

where M stands for the Earth's mass and dm is its element, δ_{ik} is the Kronecker symbol and x_j are the cartesian coordinates of dm.

We wish to investigate the variations δI_{13} and δI_{23} of the elements I_{13} and I_{23}, which define the direction of the polar axis of the Earth's inertia ellipsoid E_{in} within the coordinate system x_j. The elements I_{13} and I_{23} are related to the second-degree Stokes tesseral geopotential coefficients $J_2^{(1)}$ and $S_2^{(1)}$, also denoted as C_{21} and S_{21} and to the products of inertia D and E as follows:

$$I_{13} = -Ma_0^2\, J_2^{(1)} = -E, \tag{2}$$

$$I_{23} = -Ma_0^2 S_2^{(1)} = -D; \tag{3}$$

a_0 is the scale length factor rendering $J_2^{(1)}$ and $S_2^{(1)}$ dimensionless:

$$J_2^{(1)} = (Ma_0^2)^{-1} \int_M x_1 x_3\, \mathrm{d}m, \tag{4}$$

$$S_2^{(1)} = (Ma_0^2)^{-1} \int_M x_2\, x_3\, \mathrm{d}m. \tag{5}$$

The variations $\delta J_2^{(1)}$ and $\delta S_2^{(1)}$ also specify contributions to the changes $\delta H_1, \delta H_2$ of the Earth's spin angular momentum $\vec{H}$, which are due to the variation in the direction of the polar axis of E_{in}

$$\delta H_1 = -Ma_0^2 \omega_3 \delta J_2^{(1)}, \tag{6}$$

$$\delta H_2 = -Ma_0^2 \omega_3 \delta S_2^{(1)}; \tag{7}$$

where ω_3 is the polar component of the Earth's rotation vector $\vec{\omega}$.

The aim of this paper is to investigate, on the basis of TOPEX/POSEIDON (T/P) altimeter data (AVISO, 1999), the temporal variations of $\delta J_2^{(1)}$, $\delta S_2^{(1)}$ and their effects on the equatorial components of the Earth rotation vector (ω_1, ω_2).

2. Variations $\delta J_2^{(1)}$ and $\delta S_2^{(1)}$ Due to the Ocean Level Changes Monitored by T/P Altimetry

The T/P data covering the period Jan 1, 1993–Jan 3, 2001 (cycles 11–305) was used in the solution. The T/P data was corrected as described in Ménard et al. (1994), which includes the inverted barometer (IB) and polar tide corrections.

The geopotential model EGM96 (Lemoine et al., 1997) and sea surface topography model POCM4B (Rapp et al., 1996) were used as reference models. The same methodology was applied as described in detail Burša et al. (1999) and Burša et al. (2000), which is based on the Molodensky theory (Molodensky et al., 1960) and it allows a determination of the actual geopotential W at altimeter points independently from EGM96. In general, the determined value W differs from the geopotential W_{EGM} which is computed from EGM96. The geopotential difference

$$\delta W = W - W_{\mathrm{EGM}}, \tag{8}$$

or the corresponding radial distortions, δR, derived from δW by means of Bruns formula

$$\delta R = \frac{\delta W}{\gamma}, \tag{9}$$

where γ is the normal gravity, are then available over the ocean area S and can be represented as a series of spherical harmonics. However, because the height of the altimeter point varies during the year, consequently W, δW and δR vary, too. In this way, we can get the harmonic coefficients associated with the series of δR, which also vary in time. We did this at the time interval of three T/P cycles, i.e., approximately monthly.

In order to get the variations $\delta J_n^{(k)}$, $\delta S_n^{(k)}$, the harmonic coefficients $\delta A_2^{(1)}$ and $\delta B_2^{(1)}$ of the δR series should be inverted into the Stokes geopotential coefficients $J_n^{(k)}$, $S_n^{(k)}$. The procedure is rather laborious; it was described in Burša (1997) and we do not wish to reproduce it again. Here we are interested only in $\delta J_2^{(1)}$ and $\delta S_2^{(1)}$ for which the transformation in question is quite simple, namely

$$\delta J_2^{(1)} = \delta A_2^{(1)}/a_0, \tag{10}$$

$$\delta S_2^{(1)} = \delta B_2^{(1)}/a_0. \tag{11}$$

Note that S represents about 69% of the Earth's surface, and that the corrections due to non-orthogonality of the spherical harmonics over S, described by Burša et al. (2000), had to be introduced. Let us denote the non–orthogonality corrections to $\delta J_2^{(1)}(\delta S_2^{(1)})$ by $\varepsilon_2^{(1)}$ $(\kappa_2^{(1)})$. Then the corrections are given by

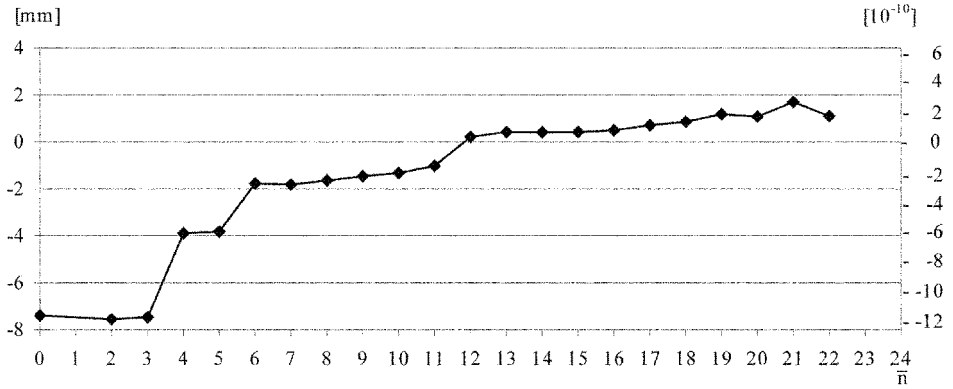

Figure 1. Correction $\epsilon_2^{(1)}$ due to non-orthogonality of harmonics over ocean area, S, as a function of the maximum of degree of harmonics retained $\bar{n}$ (in 12).

$$\begin{Bmatrix} \varepsilon_2^{(1)} \\ \kappa_2^{(1)} \end{Bmatrix} = -\left\{ \int_S \sum_{n=0}^{\overline{n}} \sum_{k=0}^{n} (w_n^{(k)} \cos k\Lambda + v_n^{(k)} \sin k\Lambda) P_n^{(k)}(\sin\phi) P_2^{(1)}(\sin\phi) \begin{matrix} \cos\Lambda \\ \sin\Lambda \end{matrix} \mathrm{d}S \right\} \times \left\{ \int_S \left[P_2^{(1)}(\sin\phi) \right]^2 \begin{matrix} \cos^2\Lambda \\ \sin^2\Lambda \end{matrix} \mathrm{d}S \right\}^{-1}, \quad (n,k) \neq (2,1); \tag{12}$$

where $w_n^{(k)}$ and $v_n^{(k)}$ are the harmonic coefficients of the spherical harmonics series for δW, $P_n^{(k)}(\sin\phi)$ is the associated Legendre function of degree n and order k, $\overline{n}$ is the maximum degree of the harmonics retained in (12), and ϕ and Λ are the geocentric latitude and longitude of $\mathrm{d}S$ and/or δW.

The corrections $\varepsilon_2^{(1)}$ and $\kappa_2^{(1)}$ depend on $\overline{n}$, the dependence is depicted in Figures 1 and 2. The left scale (in mm) is associated to $\delta A_2^{(1)}$ and $\delta B_2^{(1)}$ and the right scale (in 10^{-10}) is associated to $\delta J_2^{(1)}$ and $\delta S_2^{(1)}$ – see Equations (10) and (11).

3. Temperature Induced Variations of Mean Sea Surface

It is believed that the radial temporal variations of the ideal mean sea surface MSS, thus also of δW and δR, are mostly due to variations in the sea water density, ϱ, induced mainly by changes of the sea water temperature T within a layer of a

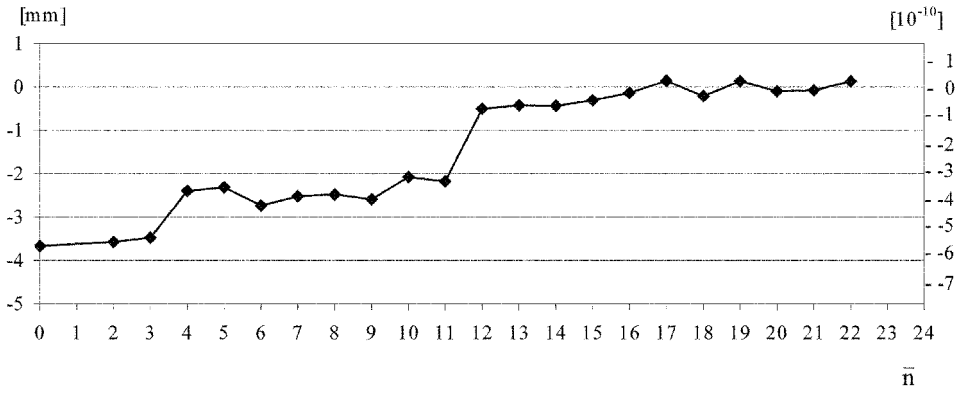

Figure 2. Correction $\kappa_2^{(1)}$ due to non-orthogonality of harmonics over ocean area, S. For $\bar{n}$ see Figure 1.

certain thickness. The density of sea water also depends on its pressure and salinity. A change in the density causes a change in height, this phenomenon is called steric sea level change.

Let us consider a thin layer of a compressible fluid with density ϱ and the free surface $z = h(x, y, t)$. A variable "liquid" volume element in the neighbourhood of the free surface contains the mass $\varrho\delta x\delta y\delta h$. The mass of the element is conserved,

$$\frac{\mathrm{d}}{\mathrm{d}t}(\varrho\delta x\delta y\delta h) = 0 \tag{13}$$

or

$$\frac{1}{\delta x\delta y}\,\frac{\mathrm{d}}{\mathrm{d}t}(\delta x\delta y) = -\frac{1}{\varrho\delta h}\frac{\mathrm{d}}{\mathrm{d}t}(\varrho\delta h)\,. \tag{14}$$

The meaning of the expression on the left side of (14) may be elucidated as follows. By differentiating we obtain

$$\frac{\mathrm{d}}{\mathrm{d}t}(\delta x\delta y) = \delta y\frac{\mathrm{d}}{\mathrm{d}t}(\delta x) + \delta x\frac{\mathrm{d}}{\mathrm{d}t}(\delta y). \tag{15}$$

The line elements δx and δy may be regarded as material elements joining adjacent particles. The stretching (or shrinking) of these elements can be due to a differential motion only. Hence

$$\frac{\mathrm{d}}{\mathrm{d}t}(\delta x) = \delta v_x = \frac{\partial v_x}{\partial x}\delta x; \quad \frac{\mathrm{d}}{\mathrm{d}t}(\delta y) = \delta v_y = \frac{\partial v_y}{\partial y}\delta y; \tag{16}$$

$$\frac{\mathrm{d}}{\mathrm{d}t}(\delta x\delta y) = \left(\frac{\partial v_x}{\partial x} + \frac{\partial v_y}{\partial y}\right)\delta x\delta y. \tag{17}$$

Obviously, an alternative form of (14) reads

$$\frac{1}{\delta x \delta y}\frac{\mathrm{d}}{\mathrm{d}t}(\delta x \delta y) = -\frac{1}{\varrho \delta h}\frac{\mathrm{d}}{\mathrm{d}t}(\varrho \delta h) = \frac{\partial v_x}{\partial x} + \frac{\partial v_y}{\partial y}. \tag{18}$$

The (horizontal) divergence of the horizontal velocity vector represents the areal expansion per unit area and unit time, and is connected with the corresponding individual changes of $\varrho \delta h$.

If the motion is nondivergent, quantity $\varrho \delta h$ is conserved following the motion. If the large-scale nondivergent motion is very slow, $\frac{\partial}{\partial t}(\varrho \delta h) \approx 0$ and then the quantity $\varrho \delta h$ is locally constant. Subject to this approximation, finite variations can be expressed as

$$\varrho \Delta(\delta h) + \delta h \Delta \varrho = 0. \tag{19}$$

If only a dependence on temperature T is considered,

$$\Delta \varrho = -\varrho_0 \alpha \Delta T. \tag{20}$$

Here ϱ_0 stands for a standard density and α is a semi-empirical coefficient of proportionality, say

$$\alpha \approx 2.5 \times 10^{-4} (^\circ\mathrm{C})^{-1}. \tag{21}$$

For details see Bryan and Cox (1967). Roughly, at $\varrho \approx \varrho_0$,

$$\Delta(\delta h) = -\frac{\delta h}{\varrho}\Delta \varrho \approx \alpha \delta h \Delta T. \tag{22}$$

The α-value of Bryan and Cox, given by (21) may be modified in a reasonable way. In reality, the coefficient of the thermal expansion is mainly a function of T with numerical values ranging, according to Chrgian (1978), from $\alpha(0^\circ\mathrm{C}) = 5.1 \times 10^{-5} (^\circ\mathrm{C})^{-1}$ to $\alpha(25^\circ\mathrm{C}) = 29.7 \times 10^{-5} (^\circ\mathrm{C})^{-1}$. However, here we have in mind density changes in a layer immediately below the ocean surface. By using (22) we arrive, with $\delta h = 40$ m and $\alpha = 10^{-4}$ $(^\circ\mathrm{C})^{-1}$, at the value

$$\frac{\Delta \delta h}{\Delta T} \approx \alpha \delta h = 4 \tag{23}$$

in [mm $(^\circ\mathrm{C})^{-1}$]. The choice of δh represents a mixed layer where the water is stirred by the wind, and roughly corresponds to typical observations of Neumann and Pierson quoted by Holland (1975). As stated by Peixoto and Oort (1991), the temperature contribution to the density field in the chosen layer is more important than salinity (in moderate latitudes). Equation (23) which is based on approximate relations (19) and (20), will be used for further evaluations.

Note that (13) produces the individual conservation of the quantity $\varrho\delta x\delta y\delta h$. Hence, the steric effect in the case of $\varrho = \varrho(T)$ may change both the form and the dimensions of the elementary liquid volume, the mass of which is conserved. Finite variations expressed by (19) represent the simplest situation resulting from the mass conservation.

Equation (18) may be written in the form

$$\frac{\partial}{\partial t}(\varrho\delta h) + \frac{\partial}{\partial x}(\varrho v_x \delta h) + \frac{\partial}{\partial y}(\varrho v_y \delta h) = 0. \tag{24}$$

Equation (24) can be integrated in the horizontal directions with respect to both cartesian coordinates over the intervals $x_B - x_A$, $y_B - y_A$, which are defining the fixed boundaries of the integration domain. The boundary conditions are prescribed by

$$\begin{aligned} v_x &= 0 \quad \text{for } x = x_A,\ x = x_B, \\ v_y &= 0 \quad \text{for } y = y_A,\ y = y_B. \end{aligned} \tag{25}$$

Thus, the normal velocity components are assumed to vanish at the boundaries. Then, by integrating (24), we obtain

$$\int_{x_A}^{x_B}\int_{y_A}^{y_B} \frac{\partial}{\partial t}(\varrho\delta h)\mathrm{d}x\mathrm{d}y = -\int_{x_A}^{x_B}\int_{y_A}^{y_B}\left[\frac{\partial}{\partial x}(\varrho v_x\delta h) + \frac{\partial}{\partial y}(\varrho v_y\delta h)\right]\mathrm{d}x\mathrm{d}y. \tag{26}$$

However, when the boundary conditions (25) are applied, the right-hand side of (26) vanishes. Hence,

$$\frac{\partial}{\partial t}\int_{x_A}^{x_B}\int_{y_A}^{y_B}(\varrho\delta h)\mathrm{d}x\mathrm{d}y = 0, \tag{27}$$

$$\int_{x_A}^{x_B}\int_{y_A}^{y_B}(\varrho\delta h)\mathrm{d}x\mathrm{d}y = \text{const}. \tag{28}$$

Equation (27) represents a generalization of the former "point" statement that quantity $\varrho\delta h$ is locally constant. Essentially, we have arrived at the mass conservation within the fixed basin defined by the above conditions.

The former relations and considerations, based on (18), will be supplemented by the general continuity equation

$$\frac{\mathrm{d}\varrho}{\mathrm{d}t} = -\varrho\left(\frac{\partial v_x}{\partial x} + \frac{\partial v_y}{\partial y} + \frac{\partial v_z}{\partial z}\right) \tag{29}$$

and by the energy equation

$$\varrho \frac{\mathrm{d}}{\mathrm{d}t}\left(\frac{1}{2}V^2 + gz\right) = \frac{\partial p}{\partial t} - \frac{\mathrm{d}p}{\mathrm{d}t}. \tag{30}$$

Here, $V^2 = v_x^2 + v_y^2 + v_z^2$, g is the mean value of the gravity acceleration and p stands for pressure. Equation (30) follows from the frictionless equation of motion (dissipative processes are excluded). By use of (29) we eliminate ϱ in (30) and we obtain the simplest combination of the both equations:

$$\left(\frac{\mathrm{d}p}{\mathrm{d}t} - \frac{\partial p}{\partial t}\right)^{-1} \frac{\mathrm{d}\varrho}{\mathrm{d}t}\frac{\mathrm{d}}{\mathrm{d}t}\left(\frac{1}{2}V^2 + gz\right) = \frac{\partial v_x}{\partial x} + \frac{\partial v_y}{\partial y} + \frac{\partial v_z}{\partial z}. \tag{31}$$

Further considerations and relations concern solely the free surface of the ocean. This surface is assumed to be a material one, formed by the same particles $\left(\frac{\mathrm{d}p}{\mathrm{d}t} = 0\right)$, while the surface pressure is allowed to vary locally $\left(\frac{\partial p}{\partial t} \neq 0\right)$. Let us go back to (18) with $\delta z = \delta h(x, y, t)$. Now, $v_z = \frac{\mathrm{d}}{\mathrm{d}t}\delta h$, $\frac{\partial v_z}{\partial z} = 0$ and (18) may be combined with (31). We find

$$\frac{\mathrm{d}}{\mathrm{d}t}\delta h = \left[\frac{\mathrm{d}}{\mathrm{d}t}\left(\frac{1}{2}V^2\right) - \frac{1}{\varrho}\frac{\partial p}{\partial t}\right]\left(\frac{1}{\delta h}\frac{\partial p}{\partial t} - g\frac{\mathrm{d}\varrho}{\mathrm{d}t}\right)^{-1}\frac{\mathrm{d}\varrho}{\mathrm{d}t}. \tag{32}$$

Equation (32) relates δh to the kinetic energy and density of the surface currents and to the atmospheric pressure in terms of the corresponding temporal changes. It is assumed that

$$\frac{1}{\delta h}\frac{\partial p}{\partial t} - g\frac{\mathrm{d}\varrho}{\mathrm{d}t} \neq 0. \tag{33}$$

Obviously, $\frac{\mathrm{d}}{\mathrm{d}t}\delta h = 0$ for $\frac{\mathrm{d}\varrho}{\mathrm{d}t} = 0$.

Comments on a detailed derivation of (32) may be found in the Appendix. Equation (32), together with the restrictive condition (33), illustrates connections between various interrelated factors. Equation (32) predicts that pressure steadiness ($\frac{\partial p}{\partial t} = 0$) excludes the direct influence of individual density changes, incorporating the steric effect.

If advective processes are very limited ($\frac{\mathrm{d}}{\mathrm{d}t} \to \frac{\partial}{\partial t}$), then (32) directly determines the local changes in the height of the free surface. Then, sea level changes in question are more pronounced when $\operatorname{sgn}\frac{\partial \varrho}{\partial t} = \operatorname{sgn}\frac{\partial p}{\partial t}$. In practice, quantity $\delta h > 0$ is the thickness of the thin elementary layer in which the density and temperature changes occur, as it is described by (22).

In agreement with the previous relations, density may now be expressed as $\varrho = \varrho_0[1 - \alpha(T - T_0)]$, ϱ_0 and T_0 being the constant reference values of density and temperature, respectively.

It is certainly useful to examine broader aspects of the steric effect expressed by $\varrho(T)$. Let us again consider the former fixed basin with the "supplementary" vertical dimension. In the simplest case, we may look at the global mass balance in a closed rectangular basin of constant depth (except for the variable free surface). We exclude the mass exchange between the ocean and atmosphere. Owing to (29), the mass conservation is generally described, in terms of the Gauss' theorem, by the relation

$$\int_{(\tau)} \frac{\partial \varrho}{\partial t} \mathrm{d}\tau = -\int_{(\sigma)} \varrho v_n \mathrm{d}\sigma, \tag{34}$$

where $\mathrm{d}\tau$ is the volume element and $\mathrm{d}\sigma$ the element of the free surface with the normal, outward directed velocity component v_n. Practically, $v_n = v_z = \frac{\mathrm{d}}{\mathrm{d}t}\delta h$. Thus, global density change obeying the "steric" relation

$$\frac{\partial \varrho}{\partial t} = -\varrho_0 \alpha \frac{\partial T}{\partial t} \tag{35}$$

and height changes of the free surface are related by (34) which is now equivalent to:

$$\varrho_0 \alpha \int_{(\tau)} \frac{\partial T}{\partial t} \mathrm{d}\tau = \int_{(\sigma)} \varrho(T) v_n \mathrm{d}\sigma. \tag{36}$$

It follows that if global decreases (increases) in ϱ prevail, the free surface tends to rise (decrease) in the mean. The right side of (34) also reflects the influence of the surface distribution of ϱ.

Naturally, the model can hardly express some important surface effects, for example, the increasing (decreasing) thickness of the surface layer in the oceanic areas of increasing anticyclonic (cyclonic) wind drag under the influence of atmospheric vortices. This has been explained in principle by J. Bjerknes (1959). On the other hand, the "steric" relation for $\varrho(T)$ is important for the energy budget in a closed basin of constant depth. For details see again Holland (1975).

The creation of vorticity or circulation is a well-known feature of flows of a fluid with nonhomogeneous density. This may be demonstrated by means of the classical theorem of V. Bjerknes. Decisive is the fact that vorticity is created (or destructed) only if the gradient of ϱ and that of p are not in the same direction. In this sense the steric effect may affect the vortex character of the flow in question.

The major problem is that there are too many interrelated factors operating in the upper layers of the ocean. This fact is reflected, to some extent, even by (32) which is less "transparent" and, consequently, less applicable than the simplified form of (18) which may be more suitable for a practical interpretation.

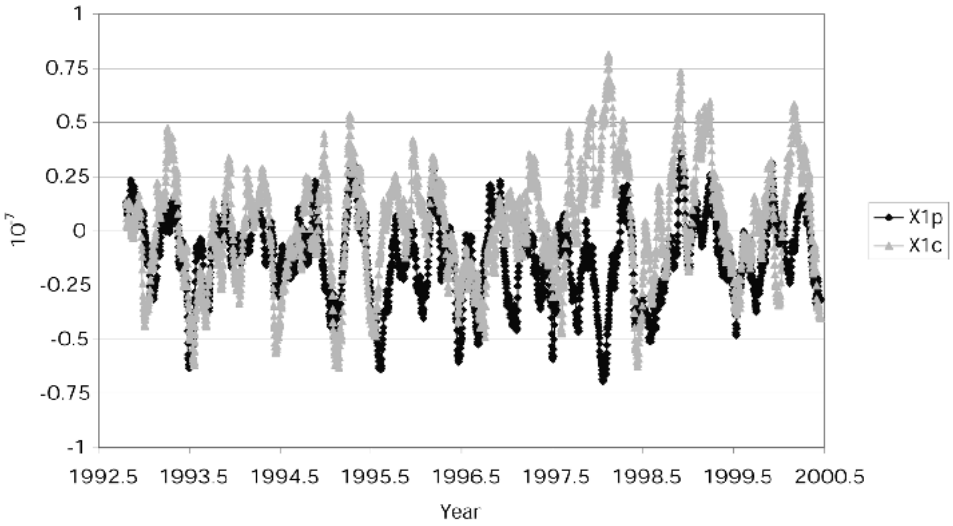

Figure 3. Pressure (mass) ($X_1 p$) and motion (current) ($X_1 c$) equatorial components of the Ocean Angular Momentum (OAM) series of Ponte and Ali (2002).

4. Altimetry Ocean Angular Momentum and Polar Motion

After accounting for sea surface topography and ocean water temperature effects as outlined in the previous section, the resulting mean sea height variations δR, observed by T/P altimetry should reflect the corresponding changes in the geopotential, provided that the altimetry measurements are properly and consistently corrected for all the necessary effects. The required altimetry corrections include, for example, instrument calibrations, propagation path delay corrections and tidal effects. After the corrections, the observed altimetry heights should reflect ocean mass distributions as well.

The oceans play an important role in the excitation of Earth's polar motion (PM) wander (i.e. the equatorial Earth rotation components ω_1, ω_2), as shown recently, e.g. by Ponte et al. (1998). Namely, after accounting for both Atmospheric Angular Momentum (AAM) and Ocean Angular Momentum (OAM) observations, most of the observed polar motion (PM) can be explained (within the correlation of about 0.80) for all periods ranging from a few days to a year (Kouba et al., 2000). While most of the explained PM effects are due to AAM, the oceans account for about 20–30% of the PM wander. Unlike the AAM PM effects, which in turn are mostly ($\sim$ 70%) caused by atmospheric mass (pressure) movements/redistribution (Barnes et al., 1983), the OAM PM effects due to the ocean mass distribution changes and ocean currents are of about equal magnitudes as can be seen in Figure 3 for the X_1 component. The X_2 component, not shown in Figure 3, has similar variations and magnitudes.

Generating OAM data is very demanding and difficult, requiring extensive numerical modelling, a number of assumptions and even external calibrations (Ponte et al., 1998). That is why only very limited OAM data is currently available and only with a considerable delay of many years. The question that then arises is to what extent a precise altimetry like from T/P, can be used to study PM, i.e. to generate the mass (pressure) portion of the OAM PM effects. The mass portion of OAM was found to be largely responsible for excitation of Chandler wobble (Gross, 2000).

We follow the classical developments of Barnes et al. (1983), while accounting for the International Earth Rotation Service (IERS) convention for the PM coordinates x, y with respect to the Earth equatorial rotation vector components ($\omega_1 = m_1\omega = x\omega$; $\omega_2 = m_2\omega = -y\omega$). Neglecting the second order terms, the Liouville equation, which relates PM, PM rates ($\dot{x}, \dot{y}$) and the excitation functions (X_1, X_2), becomes (Barnes et al., 1983):

$$\dot{x} - y\omega_{\mathrm{ch}} = X_2\omega_{\mathrm{ch}}, \tag{37}$$

$$\dot{y} + x\omega_{\mathrm{ch}} = X_1\omega_{\mathrm{ch}}, \tag{38}$$

where $\omega_{\mathrm{ch}} = 2\pi/434$ day^{-1} is the Chandler wobble (CW) rotational velocity. Note that, the small terms accounting for CW damping have been neglected here, consistently with Barnes et al. (1983). The expression on the left-hand sides of (37) and (38) can be interpreted as the PM rates in excess of CW, and will be referred to here as the "excess" PM rates. Then, according to (37) and (38), the excess PM rates should be proportional to the excitation functions.

In the absence of external torques, the effective excitation functions, which take into account (i.e. they are in addition to) the changes of the gravitational potential due to PM, so called the polar tides as well as the tidal loading deformations of the geopotential surface, then are:

$$X_1 = \frac{\frac{k_0(1+\dot{k}_2)}{(k_0-k_2)}(\Delta I_{13} + \Delta\dot{I}_{23}/\omega) + \frac{k_0}{(k_0-k_2)}(h_1/\omega + \dot{h}_2/\omega^2)}{C - A}, \tag{39}$$

$$X_2 = \frac{\frac{k_0(1+\dot{k}_2)}{(k_0-k_2)}(\Delta I_{23} - \Delta\dot{I}_{13}/\omega) + \frac{k_0}{(k_0-k_2)}(h_2/\omega - \dot{h}_1/\omega^2)}{C - A}. \tag{40}$$

Here $\omega = \omega_3$ is the Earth rotation rate; $(C - A)$ is the well known difference of the principal inertia moments and h_1, h_2 are the angular moments due to relative motions. The coefficients $k_0 = 0.938$, $\dot{k}_2 = -0.308$ and $k_2 = 0.298$ are the secular, the second degree loading and the rotational Love numbers, respectively (Burša and Kostelecký, 1999). After substitutions of the above values into (39) and (40), the effective excitation functions become:

$$X_1 = \frac{1.01(\Delta I_{13} + \Delta\dot{I}_{23}/\omega) + 1.46(h_1/\omega + \dot{h}_2/\omega^2)}{C - A}, \tag{41}$$

$$X_2 = \frac{1.01(\Delta I_{23} - \Delta \dot{I}_{13}/\omega) + 1.46(h_2/\omega - \dot{h_1}/\omega^2)}{C - A}. \tag{42}$$

The first two terms on the right hand side of (41) and (42) include inertia tensor changes, thus are caused by mass (pressure) distribution, while the last two terms involve velocities and are caused by relative motions (ocean currents). Only the mass (pressure) OAM components should be observable by altimetry, since the altimetry data cannot infer subsurface ocean currents, which are essential for the velocity component of OAM. Furthermore, since for AAM the terms with the inertia tensor rates $\Delta \dot{I}$ are two orders of magnitude smaller than the first term containing $\Delta \dot{I}$ (Barnes et al., 1983), thus they should also be equally small for OAM and can be safely neglected. Consequently, the altimetry observations, after the appropriate corrections, should be able to yield the mass portion of the OAM PM effects. Then, the mass OAM effective excitation functions could be evaluated in the following form:

$$X_1 = \frac{1.01\ \Delta I_{13}}{C - A}, \tag{43}$$

$$X_2 = \frac{1.01\ \Delta I_{23}}{C - A}. \tag{44}$$

From (2) and (3), which relate the inertia element variations (ΔI_{13}, ΔI_{23}) to the changes of the second degree tesseral geopotential coefficients ($\delta J_2^{(1)}$, $\delta S_2^{(1)}$), and from (10) and (11), after the substitutions for the second degree zonal geopotential coefficient $J_2 = (C - A)/(Ma_0^2)$, one obtains the final form of the mass portions of the OAM effective excitation functions, which are evaluated solely from altimetry observations of the radial distortion coefficients ($\delta A_2^{(1)}$, $\delta B_2^{(1)}$):

$$X_1 = \frac{-1.01\ \delta A_2^{(1)}}{a_0 J_2}, \tag{45}$$

$$X_2 = \frac{-1.01\ \delta B_2^{(1)}}{a_0 J_2}, \tag{46}$$

These, after the substitution of $J_2 = 1.0826359 \times 10^{-3}$ (McCarthy, 1996) are equal to

$$X_1 = -933\ \delta J_2^{(1)} = -933\ \delta A_2^{(1)}/a_0, \tag{47}$$

$$X_2 = -933\ \delta S_2^{(1)} = -933\ \delta B_2^{(1)}/a_0. \tag{48}$$

Since the effective excitation functions (X_1, X_2) are formulated without the polar tides, by using the effective coefficients of (39) and (40), then the altimetry

height observations, or alternatively, the derived second degree tesseral Stokes coefficients ($J_2^{(1)}$, $S_2^{(1)}$), must also be corrected for polar tide effects. The polar tide corrections can be easily computed from the PM departures from the mean pole ($x - \bar{x}$; $y - \bar{y}$):

$$\Delta J_2^{(1)} = \frac{+k_2\omega^2 a_0^3}{3GM}(x - \bar{x}), \tag{49}$$

$$\Delta S_2^{(1)} = \frac{-k_2\omega^2 a_0^3}{3GM}(y - \bar{y}). \tag{50}$$

The polar tide theory and application can be find, e.g., in McCarthy (1996).

5. Results

The temporal variations $\delta J_2^{(1)}$ and their analytical expressions (with the annual and semi-annual terms) for years 1993–2000 are depicted in Figures 4 and 5. The analytical expressions are incorporated into each figure. The expressions were obtained by a least square fit to the observed data. The rms errors are given also in each analytical term connected with the fit. The observed data is marked by ■ in all figures.

Analogously, the corresponding temporal variations of $\delta S_2^{(1)}$ are shown in Figures 6 and 7. Since we are interested in the steric corrections of the second-degree tesseral harmonic Stokes geopotential coefficients, we also require the corresponding tesseral harmonic terms of the ocean surface temperature series. The temperature harmonic terms $Y_2^{(1)}$ and $Z_2^{(1)}$ (also with the annual and semi-annual fitting curves) are depicted in Figures 8 and 9, and in Figures 10 and 11, respectively. They were computed from the temperature data of the ocean surface water (taken from http://podaac-www.jpl.nasa.gov/sst/). In some cases the semi-annual terms can hardly be considered statistically significant.

A relatively high correlation ($r \approx 0.9$) was found between the annual terms of $\delta J_2^{(1)}$ and $Y_2^{(1)}$ and between the annual terms of $\delta S_2^{(1)}$ and $Z_2^{(1)}$ (see Figures 4–11). That is why, the simple steric corrections (23) were introduced for the $\delta J_2^{(1)}$ and $\delta S_2^{(1)}$ series shown in Figure 12. The height temperature coefficient of $\frac{\Delta\delta h}{\Delta T} = 4$ mm/°C, which according to (23) corresponds to a water layer thickness of only 40 m, has resulted in the smallest rms variations of the temperature corrected series of $\delta J_2^{(1)}$ and $\delta S_2^{(1)}$. However, a more rigorous steric correction treatment requires an integration of several ocean water layers reaching a depth of up to several hundred meters (Chen et al., 1998).

Also shown in Figure 12 are the polar tide corrections (49) and (50), in order to verify that indeed these corrections were applied in preprocessing of altimetric data (Ménard et al., 1999). As one can see, the pole tide effects are of the same

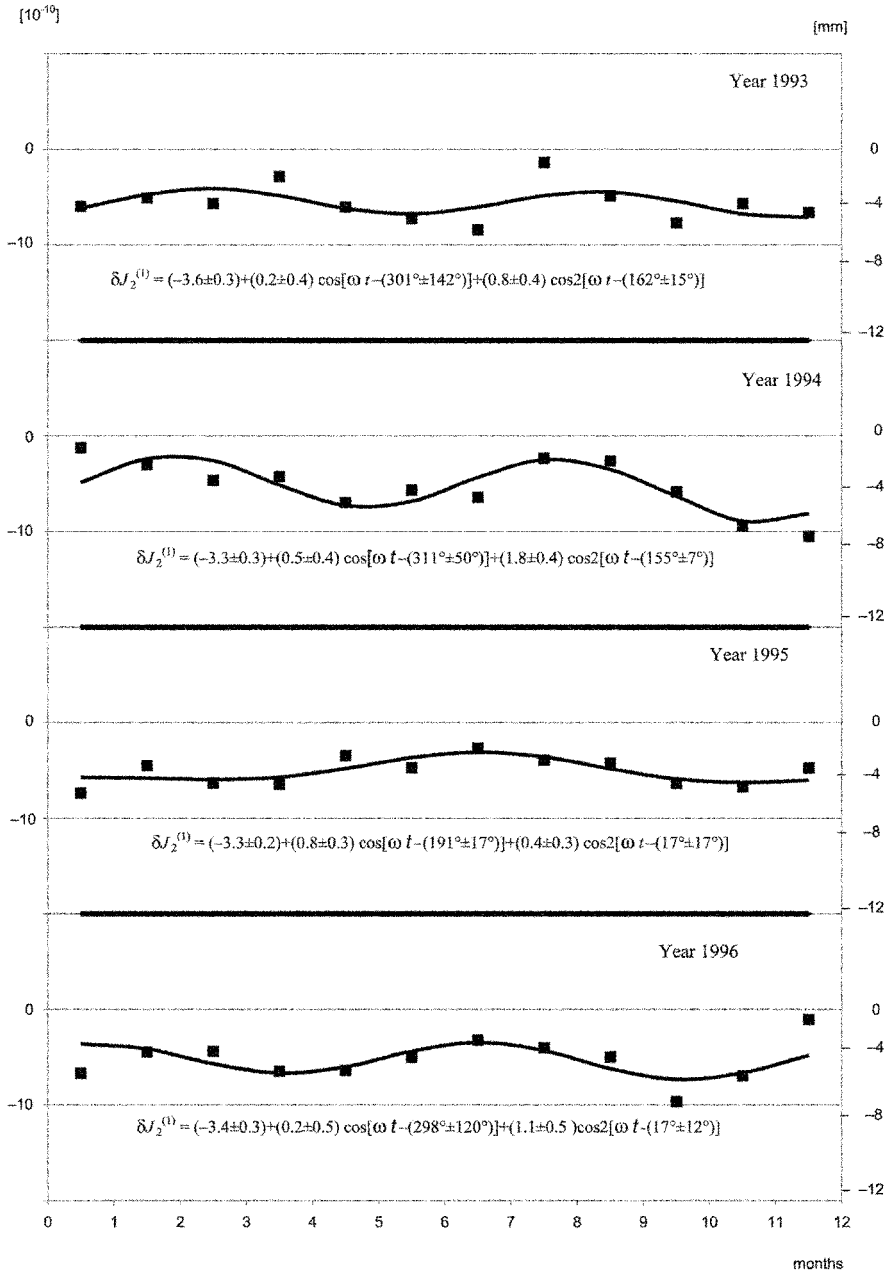

Figure 4. Seasonal variations in the Stokes geopotential coefficient $\delta J_2^{(1)}$ of the mean sea surface, 1993–1996.

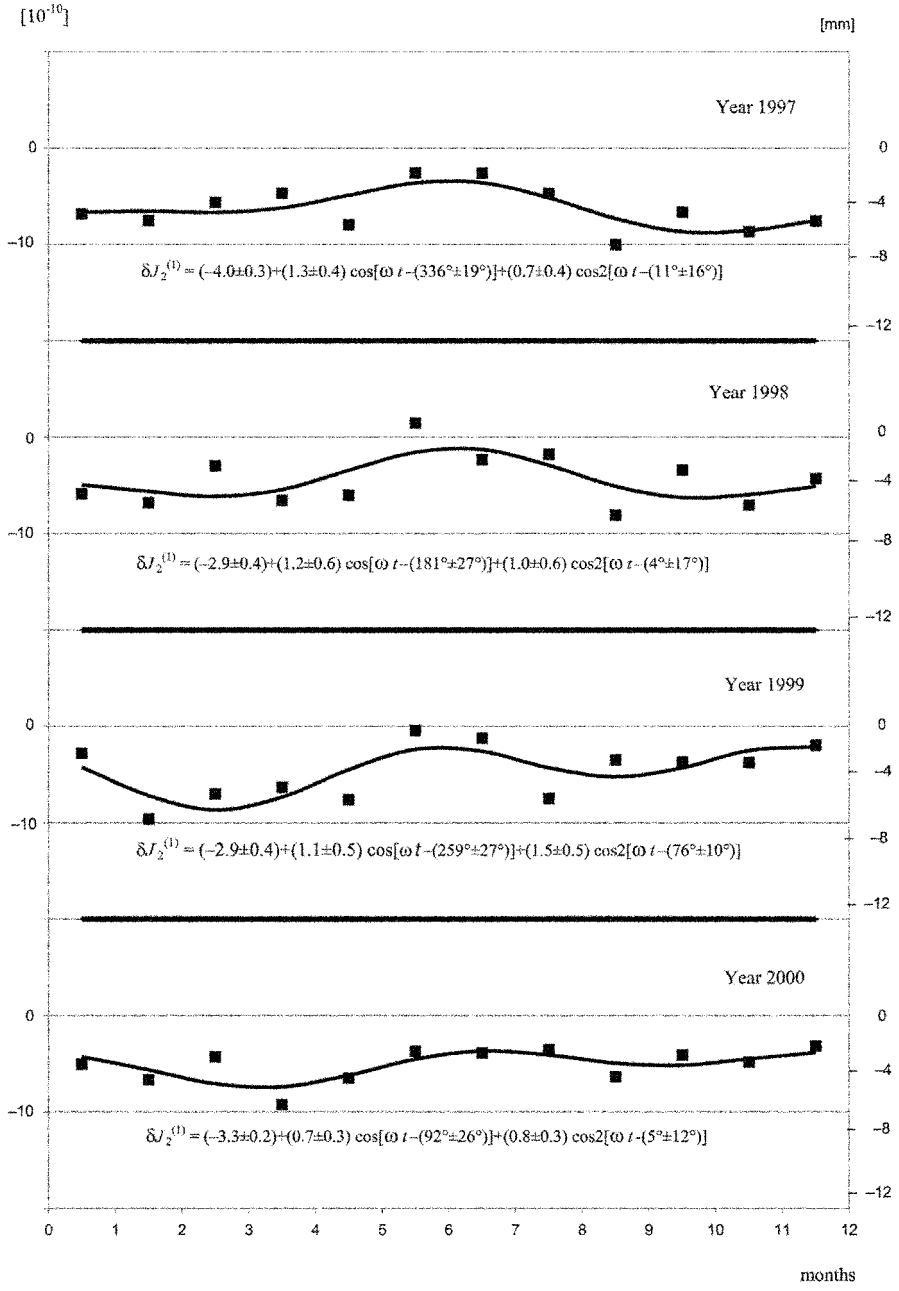

Figure 5. Seasonal variations in the Stokes geopotential coefficient $\delta J_2^{(1)}$ of the mean sea surface, 1997–2000.

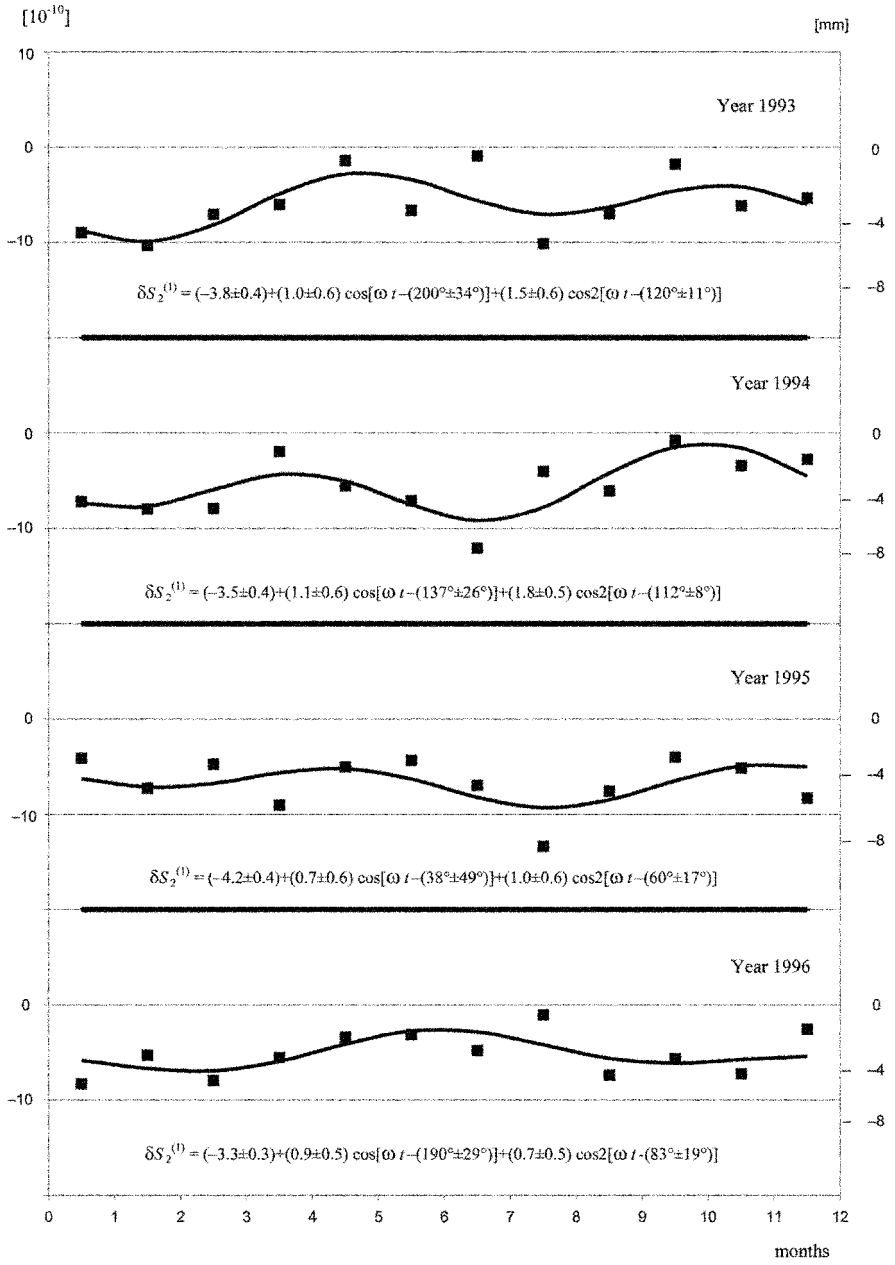

Figure 6. Seasonal variations in the Stokes geopotential coefficient $\delta S_2^{(1)}$ of the mean sea surface, 1993–1996.

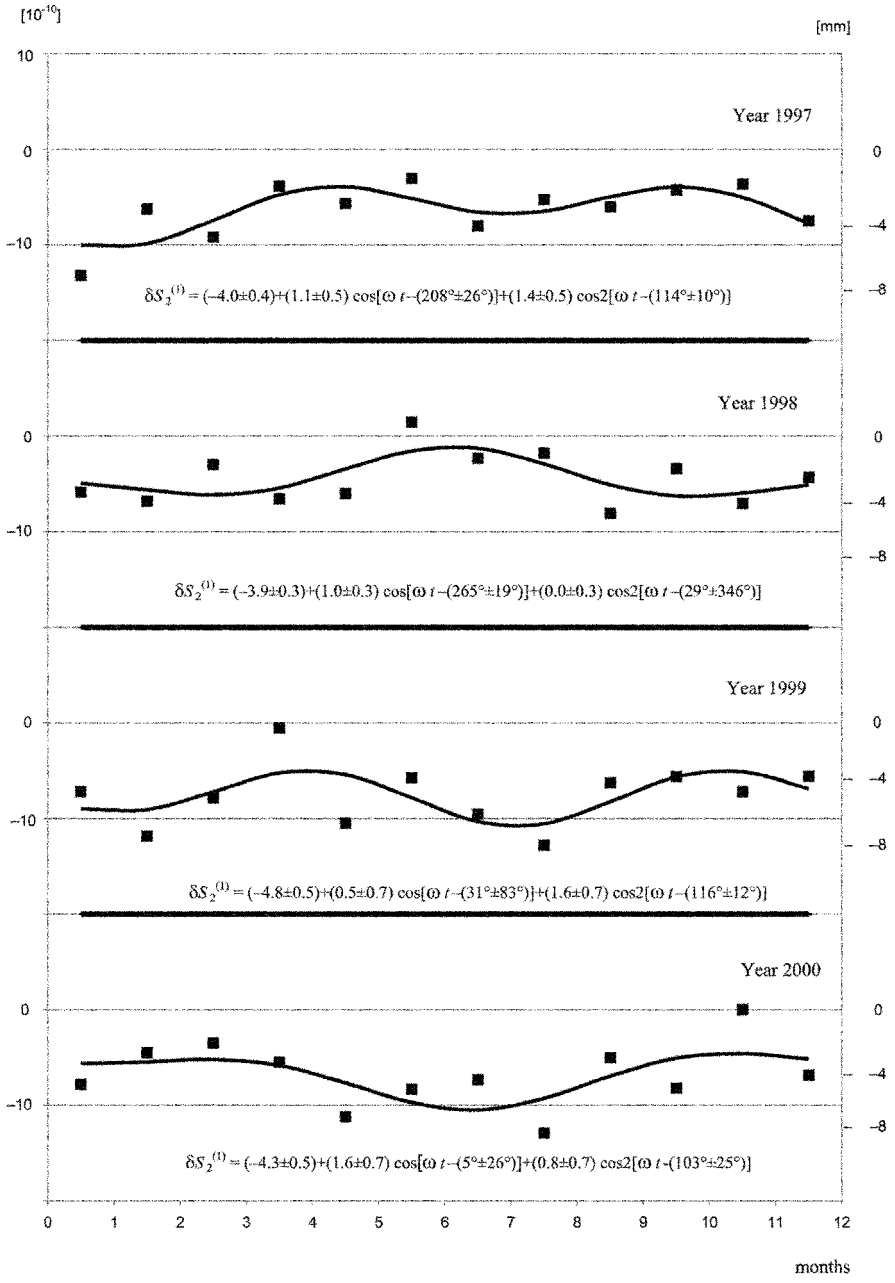

Figure 7. Seasonal variations in the Stokes geopotential coefficient $\delta S_2^{(1)}$ of the mean sea surface, 1997–2000.

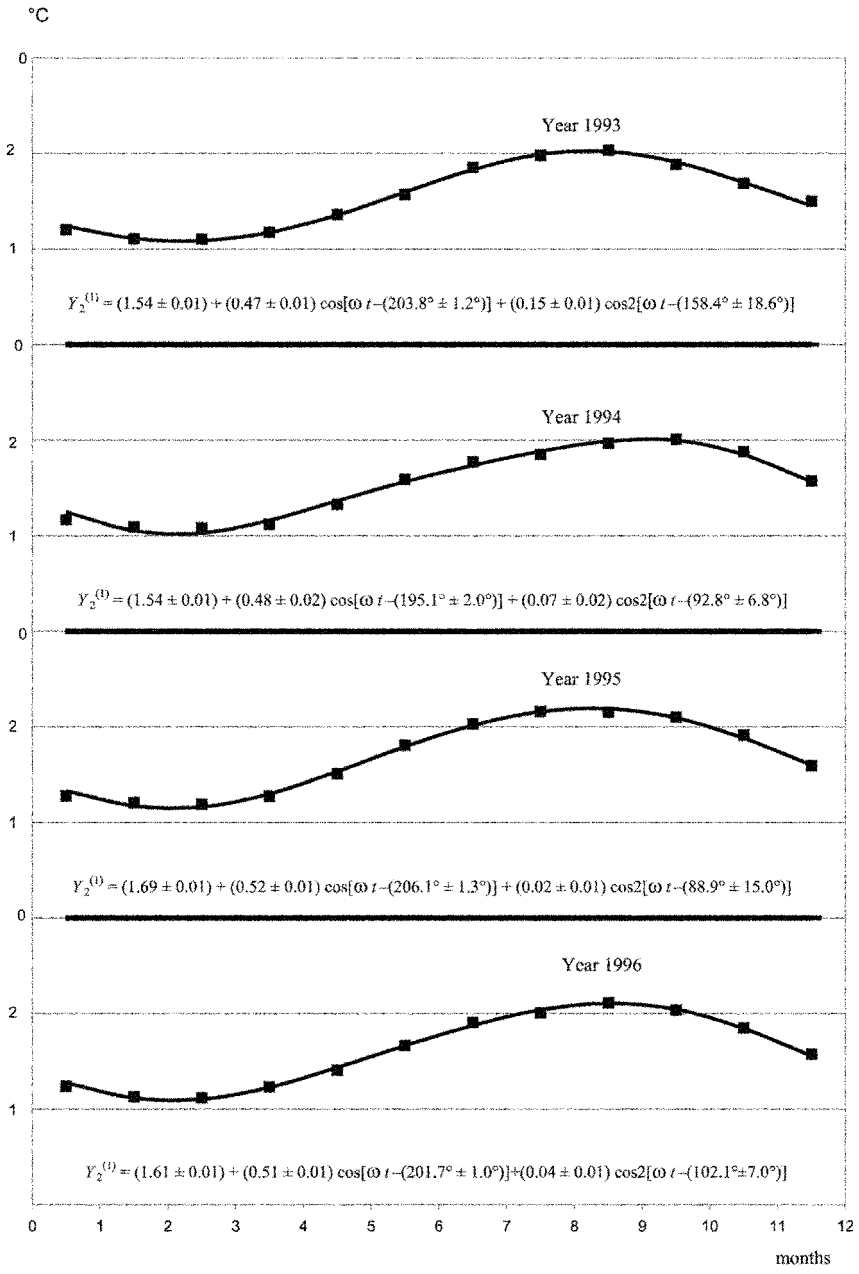

Figure 8. Seasonal variations in the sea surface temperature harmonic term $Y_2^{(1)}$, 1993–1996.

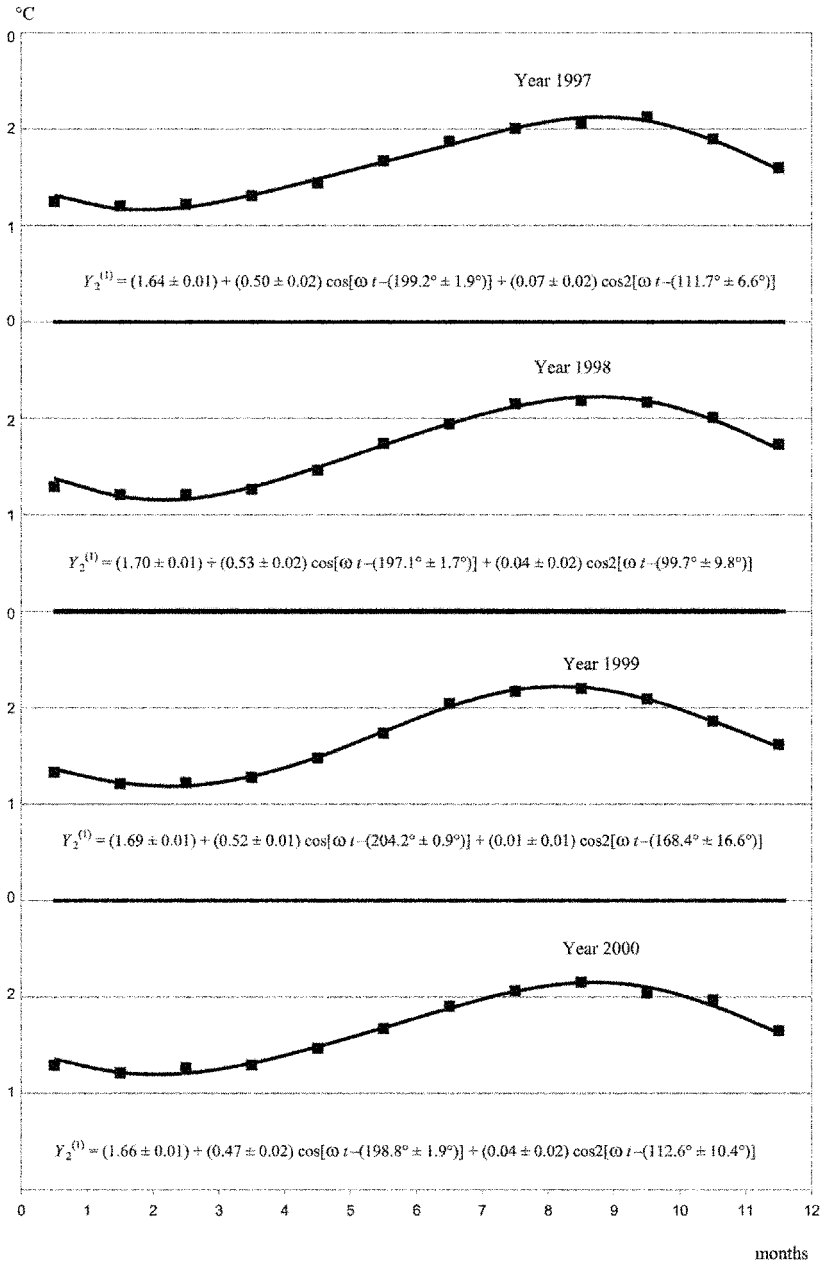

Figure 9. Seasonal variations in the sea surface temperature harmonic term $Y_2^{(1)}$, 1997–2000.

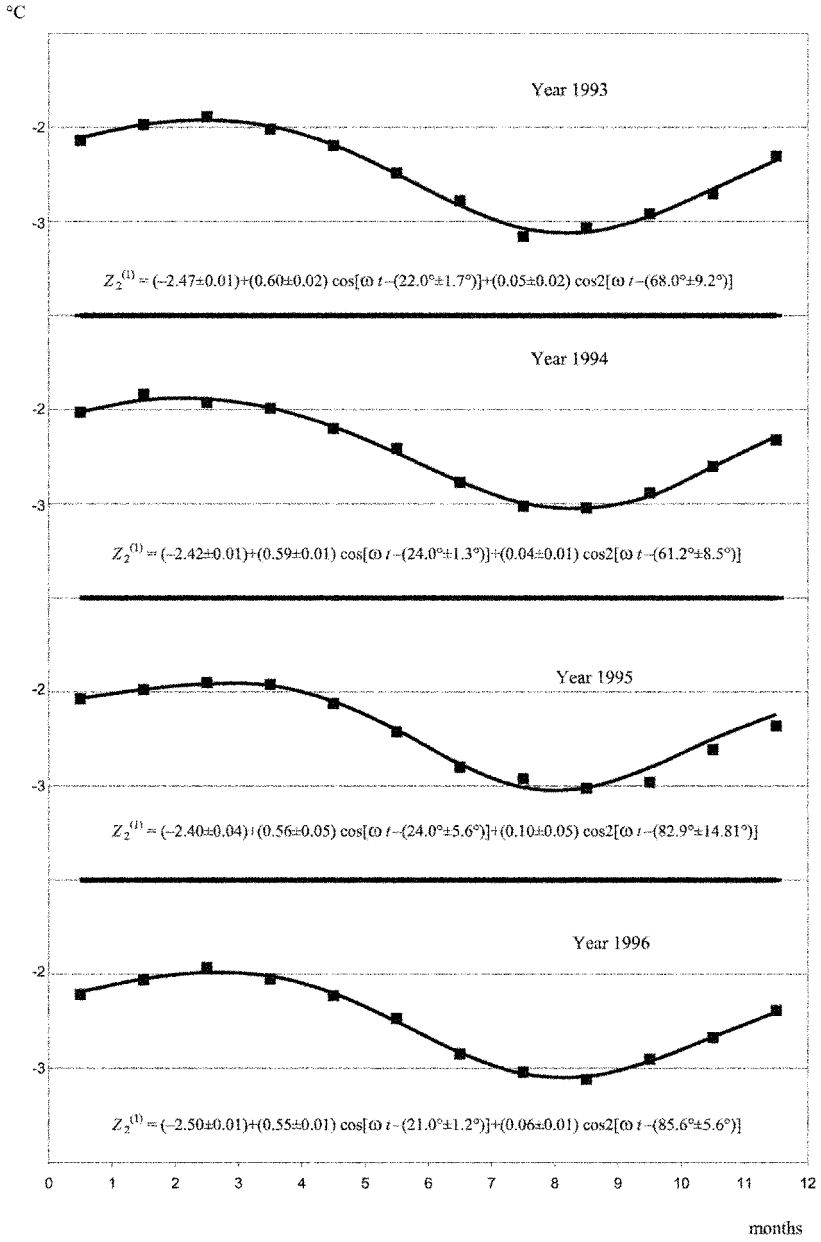

Figure 10. Seasonal variations in the sea surface temperature harmonic term $Z_2^{(1)}$, 1993–1996.

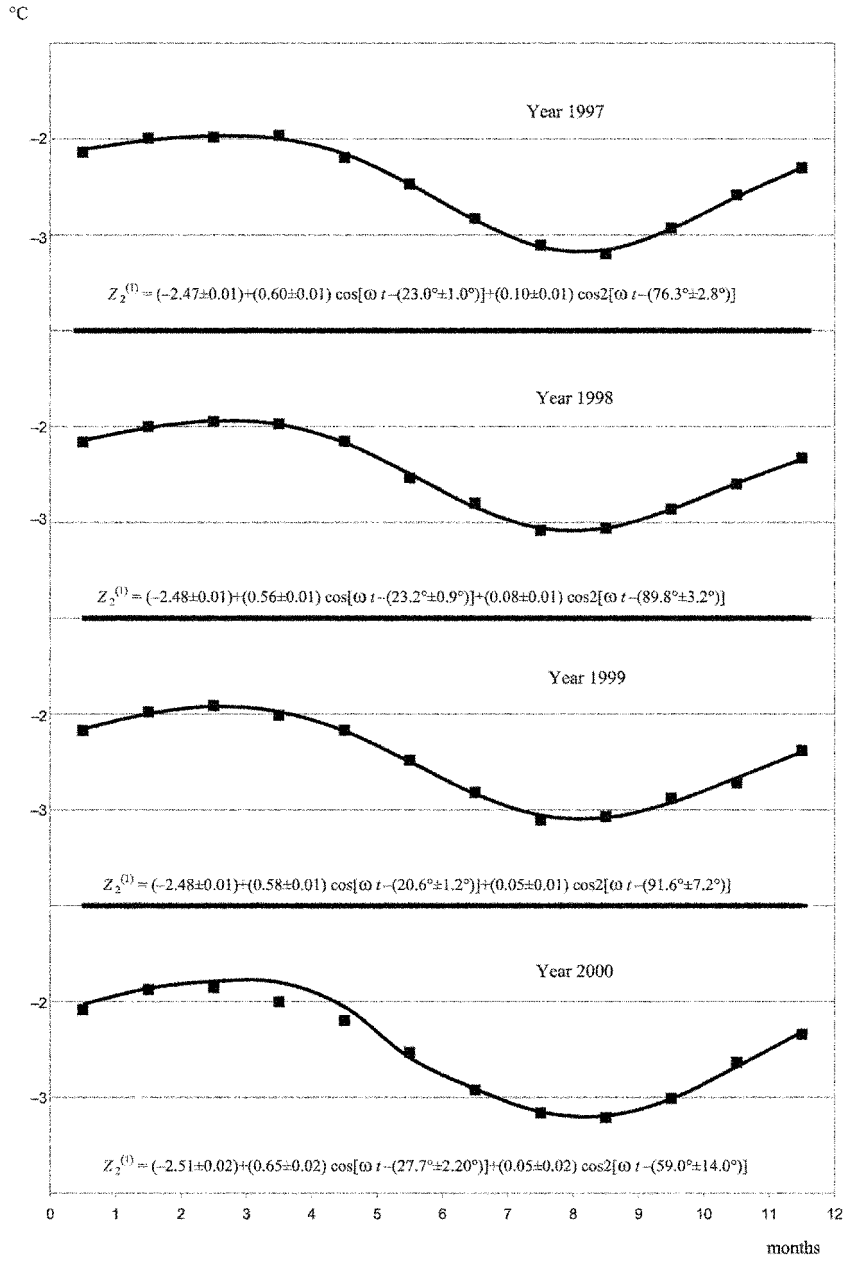

Figure 11. Seasonal variations in the sea surface temperature harmonic term $Z_2^{(1)}$, 1997–2000.

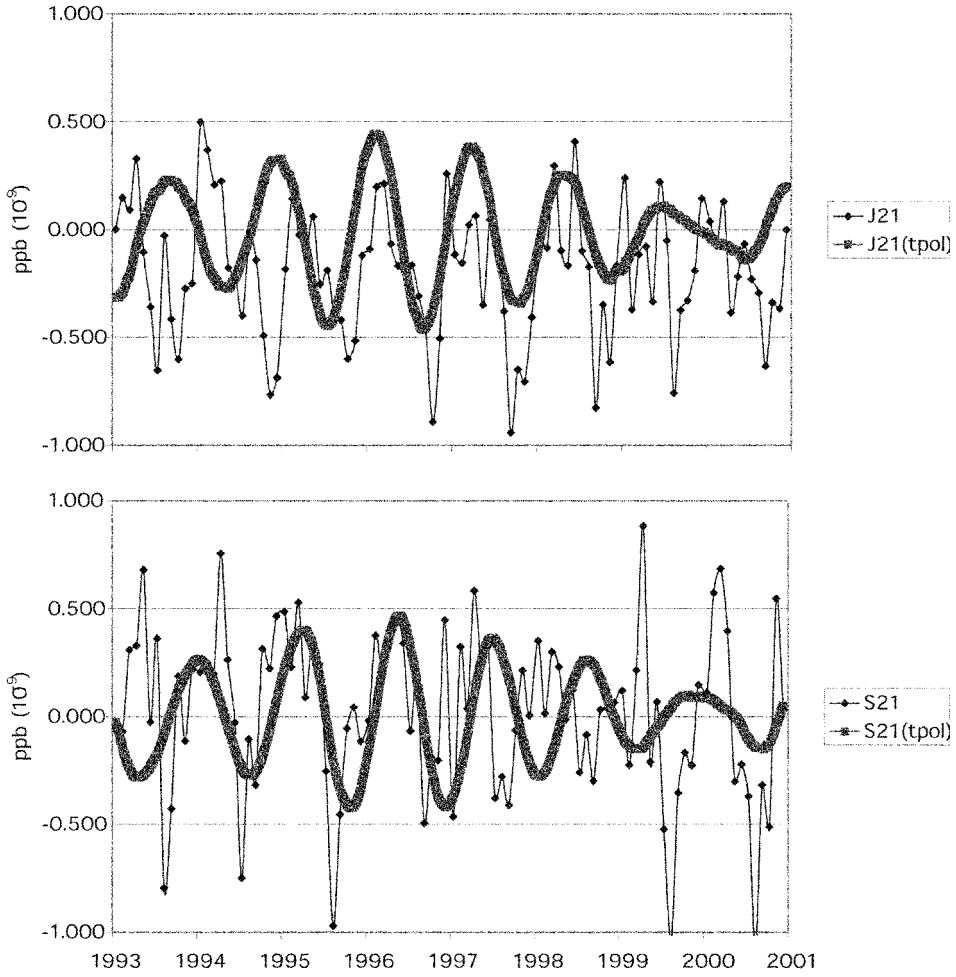

Figure 12. The second degree tesseral geopotential coefficients ($\delta J_2^{(1)}$, $\delta S_2^{(1)}$) corrected for steric temperature effects with 4 mm/°C and the corresponding pole tide corrections (*tpol*) evaluated according to (49) and (50).

amplitude as the observed variations of ($\delta J_2^{(1)}$, $\delta S_2^{(1)}$), i.e. with amplitudes of about 0.5 ppb ($\sim$ 3 mm) and there is no significant correlation or coherence between the two series, thus indicating that the polar tide corrections were indeed applied in preprocessing.

The mass portion of the OAM effective excitation functions, which can also be derived from T/P data, is expected to be significant, perhaps accounting for more than 50% of the OAM PM effects. Then, the observed excess PM rates given by (37), (38) (after subtracting the AAM PM effects) should be similar to the T/P derived effective excitation functions in (47) and (48) after multiplying by ω_{ch}. The precision of the monthly determinations of the δR harmonic coefficient is about

2 mm (0.3 ppb), which is consistent with T/P altimetry height precision of 2 cm, and it corresponds to an orientation change of the Earth polar axis and its rate of about 60 milli arc sec (mas) and 0.9 mas/day, respectively. For the interval used in this analysis, this precision implies formal solution sigmas of about 0.1 mas/day for the amplitudes of the semi-annual and longer periods. That is why one should expect to detect from T/P altimetry only the OAM PM signals at the semi-annual and longer periods.

Figure 13 confirms the expected high noise of the excess PM rates derived from T/P. Figure 13 also shows the precise excess PM rates obtained from the complete (pressure + velocity) OAM series (Ponte and Ali, 2002) and the IERS Bulletin A excess PM rates corrected for AAM. The AAM used here was based on the reanalysis of the U.S. National Centers for Environmental Prediction and it was obtained from the IERS Special Bureau for Atmosphere (Salstein and Rosen, 1997). In Figure 13, all the three series include the IB corrections. Furthermore, the OAM and Bulletin A PM rates, which have daily sampling, were smoothed with a 30 day running mean to be compatible with the monthly T/P averages. The high correlation ($r \approx 0.8$ for both PM components) between the Bulletin A residual (*a-aam*) and the OAM (*oam*) series during this interval is clearly seen in Figure 13.

Figure 14 summarizes the spectral analysis (prograde and retrograde amplitudes) of the excess PM rates for the above IERS Bulletin A, corrected for AAM (*A-aam*) along with the T/P (*T/P*) and the OAM PM rate effects (*Oam*). Additionally the pressure OAM (*Op*), which should be the same as the (*T/P*) series, is also shown here.

As one can readily seen in Figure 14, there is a little or no similarity between the "noisy" T/P with the (*A-aam*), (*Oam*) and the (*Op*) signals. Note that the expected formal sigmas of 0.1 mas/day for the T/P amplitudes at the semi-annual and longer periods are hardly sufficient for the detection of the (pressure) OAM effects, since the (*Op*) amplitudes seen in Figure 14 are well below the noise level of T/P amplitudes. The high degree of agreement between the OAM (*Oam*) and the Bulletin A residuals (*A-aam*) series is clearly seen in Figure 14 for all periods, in particular for the annual, semiannual (1, 2 cy/y) and the Chandler (prograde 0.84 cy/y) periods. However, even the above maximum peaks are hardly above the noise level of the T/P spectrum. It is interesting to note that in Figure 14 the largest amplitude peak is seen for the Bulletin A/AAM residuals (*A-aam*) at the CW period which is also well reflected by a large CW peak in the OAM (*Oam*). This is quite consistent with Gross (2000), where it was concluded that a majority of CW could be accounted for by OAM.

The IB correction model may be considered problematic for altimetry analyses, however the most precise PM observations inequitably favour the IB corrections of AAM data. For example, the rms agreement between the observed excess PM rates and the ones derived from AAM with the IB model corrections, decreased from 0.6 mas/d down to 0.3 mas/d. Furthermore, the correlation of the IB corrected AAM with the observed PM rates was always significantly better with the IB corrections

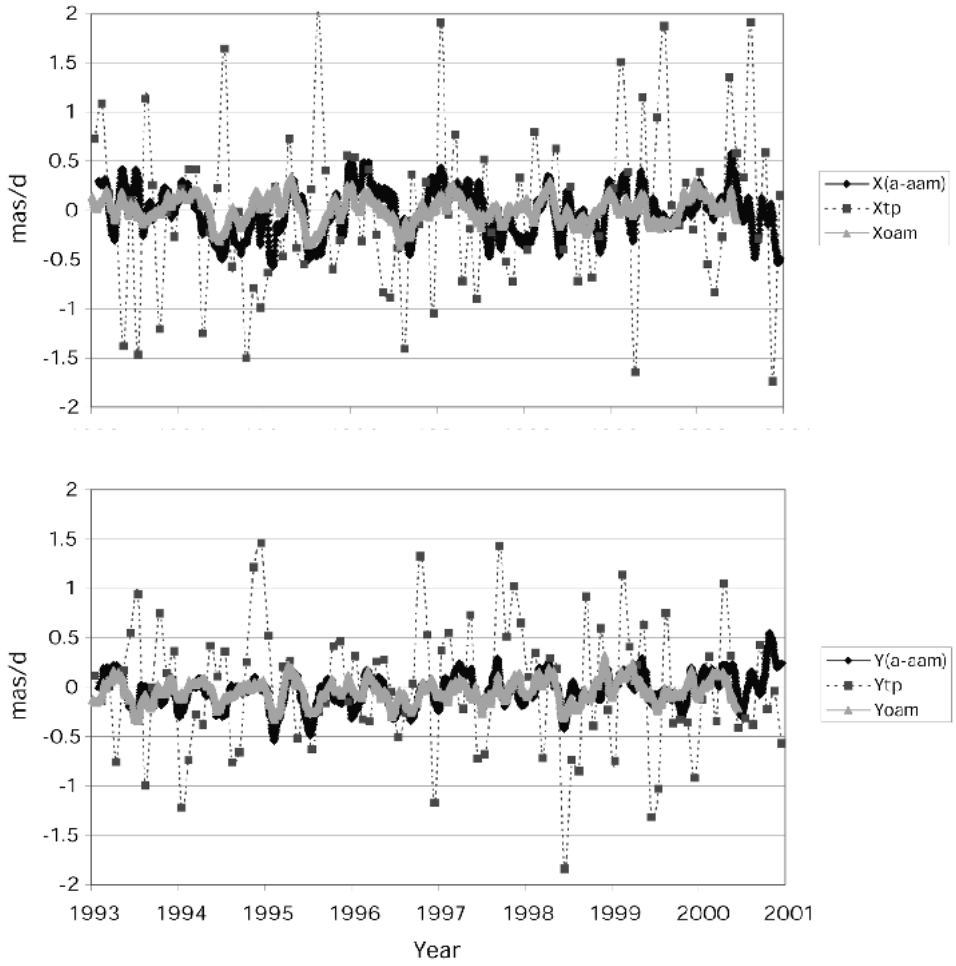

Figure 13. Excess PM x, y rates: (*a-aam*) – IERS Bull. A corrected for AAM; *tp*) – derived from T/P; (*oam*) – derived from OAM.

than with no IB corrections. This was true for all periods longer than six days (Kouba et al., 2000). The same conclusion was also reached here for the IERS Bulletin A PM observations during the period of 1993–2000. This is a significant finding, since PM observations represent an objective global criterion that is free of any calibration and/or model assumptions. In fact, the Earth rotation represents a precise and global integrator of the complete Earth's energy regime. Consequently, the application of IB corrections should also be justified for altimetry data, and that is why it was also used here.

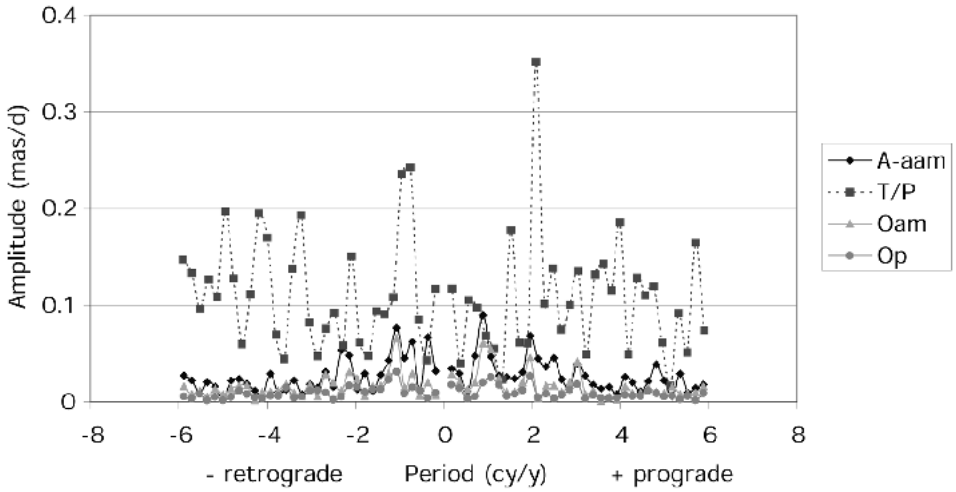

Figure 14. Retrograde (−) and prograde (+) amplitudes for the excess PM rates: (*A-aam*) – IERS Bull. A corrected for AAM; (*T/P*) – derived from T/P; (*Oam*) – derived from (pressure+ velocity) OAM and (*Op*) from pressure OAM.

6. Conclusions

T/P altimetry data was used to monitor, at about 0.3 ppb (10^{-9}) precision level, the variations of the second order tesseral geopotential coefficients, which describe the orientation of polar axis orientation of the Earth inertia ellipsoid. The temperature dependence of the mean sea level heights was described and applied in order to derive realistic variations of the tesseral geopotential coefficients. The suitability of the derived tesseral coefficients for the derivation of the pressure component of Ocean Angular Momentum (OAM) was also investigated. The noise level of the OAM excess PM rate components derived from T/P tesseral geopotential coefficients was found to be significantly larger than the OAM PM effects based on oceanic data and models. The oceanic OAM PM effects compared quite well with the precise PM observations, once the Atmospheric Angular Momentum data were taken also into account. The large noise/amplitudes of the T/P derived OAM solutions should be further investigated.

Acknowledgements

The Ponte and Ali (2002) OAM daily series was kindly provided by R. E. Ponte of Atmospheric and Environment Research, Inc., Lexington. Mass., USA. The authors wish to express sincere thanks to the anonymous reviewer for his valuable comments.

7. Appendix

Pressure continuity at the free surface.

The particles close to the ideal free surface will follow this surface during its motion. Pressure is invariably continuous at the surface. The large-scale "smoothed" oceanic pressure field p_0 may be described by the simple, so called inverted barometer (IB), hydrostatic formula

$$p_0 = p_A + g \int_Z^0 \varrho \mathrm{d}z \tag{51}$$

which relates p_0 to the variable atmospheric surface pressure p_A. Here, $z = 0$ corresponds to the equilibrium free surface (in other words, z is now the distance downward from the ocean surface and the depth varies from z to zero at the surface). The departures of the actual free surface from the equilibrium state are assumed to be small. Hence, pressure continuity may be prescribed at $z = 0$ where $p_0 = p_A$. At the material free surface we must have $\frac{\mathrm{d}p_0}{\mathrm{d}t} = 0$. Consequently, $\frac{\mathrm{d}p_A}{\mathrm{d}t} = 0 = \frac{\partial p_A}{\partial t} + \overrightarrow{v}_A \cdot \nabla p_A$. Thus, local pressure changes are associated solely with the advection due to the large-scale wind vector $\overrightarrow{v}_A$ which is generally ageostrophic:

$$\frac{\partial p_A}{\partial t} == -\overrightarrow{v}_A \cdot \nabla p_A. \tag{52}$$

This pressure tendency operates in (32) where the subscript A has been omitted. Note that the geostrophic approximation for the wind vector would result in $\frac{\partial p_A}{\partial t} = 0$.

Let us integrate the energy relation (30) over the former basin with rigid walls and a variable free surface. Owing to the assumptions used, the basin represents a "liquid" volume formed by the same water particles. The variability of this volume is reflected by the changes of its free surface. Now,

$$\begin{aligned} \frac{\mathrm{d}E}{\mathrm{d}t} &= -\int_{(\sigma)} p v_n \mathrm{d}\sigma + \int_{(\tau)} p \left(\frac{\partial v_x}{\partial x} + \frac{\partial v_y}{\partial y} + \frac{\partial v_z}{\partial z} \right) \mathrm{d}\tau \\ &= -\int_{(\sigma)} p v_n \mathrm{d}\sigma - \int_{(\tau)} \frac{p}{\varrho} \frac{\mathrm{d}\varrho}{\mathrm{d}t} \mathrm{d}\tau. \end{aligned} \tag{53}$$

Symbol E stands for the total mechanical (kinetic + potential) energy in the liquid volume in question. For the derivation and interpretation of (53) see, for example, Brdička (1959). The volume integral on the right side of (53) includes the steric effect. Further,

$$\int_{(\sigma)} p v_n \mathrm{d}\sigma = \int_{(\sigma)} p_A v_n \mathrm{d}\sigma \tag{54}$$

by virtue of the pressure continuity at the free surface. By and large, (53) represents, to some extent, an energetical interpretation of the steric effect. Decreases in ϱ contribute to the increase of E. The role of the atmospheric pressure is underlined, too. Atmospheric pressure now operates, in agreement with (34), against the steric effect.

Obviously, the validity of these statements is limited by various simplifying assumptions.

References

AVISO/CALVAL yearly Report: 1999, 'TOPEX/POSEIDON Cycles 1 to 231(1993–1999)', AVI-NT-O11-316-CN Edition 1,0, 66 pp.

Barnes, R. T. H., Hide, R., F.R.S., White, A. A., and Wilson, C. A.: 1983, 'Atmospheric Angular Momentum Fluctuations, Length-of-day Changes and Polar Motion', *Proc. Roy. Soc. Lond.*, Ser. A, **387**, 31–73.

Bjerknes, J.: 1959, 'The Recent Warming of the North Atlantic', in B. Bolin (ed.), *The Atmosphere and the Sea in Motion*, The Rossby Memorial Volume. pp. 65–73, New York, The Rockefeller Institute Press, Oxford University Press, 509 pp.

Brdička, M.: 1959, 'Mechanics of Continuous Media', pp. 408–409, (in Czech), *NČSAV*, Praha, 718 pp.

Bryan, K. and Cox, M. D.: 1967, 'A Numerical Investigation of the Oceanic General Circulation', *Tellus* **19** (1).

Burša, M.: 1997, 'Converting Radial Distortions due to Geopotential Models to Geopotential Stokes Coefficients', *Studia geoph. et geod.* **41**, 407–415.

Burša, M., Kouba, J., Raděj, K., True, S. A., Vatrt, V., and Vojtíšková, M.: 1999, 'Temporal Variations in Sea Surface Topography and Dynamics of the Earth's Inertia Ellipsoid', *Studia geoph. et geod.* **43**, 7–19.

Burša, M. and Kostelecký, J.: 1999, *Space Geodesy and Space Geodynamics*, Ministry of defence of the Czech Republic, Prague, 455 pp.

Burša, M., Kouba, J., Vatrt, V., Vítek, V., and Vojtíšková, M.: 2000,'Topex/Poseidon Altimetry and Dynamics of the Ocean–atmosphere system', *Studia geoph. et geod.* **44**, 1–12.

Cabanes, C., Cazenave, A., Le Provost, C.: 2001, 'Sea Level Changes from TOPEX/POSEIDON Altimetry for 1993–1999, and Warming of the Southern Oceans', *Geophys. Res. Lett.* **28**, 9–12.

Cazenave, A., Dominh, K., Soudarin, L., Ponchaut, F., and Le Provost, C.: 1999, 'Sea Level Changes from TOPEX/POSEIDON Altimetry and Tide Gauges, and Vertical Crustal Motions from DORIS', *Geophys. Res. Lett.* **26**, 2077–2080.

Cazenave, A., Remy, F., Dominh, K., and Douville H.: 2000, 'Global Oceans Mass Variation, Continental Hydrology and the Mass Balance of the Antarctica Ice Sheet at Seasonal Time Scale', *Geophys. Res. Lett.* **27**, 3755–3758.

Chambers, D. P., Chen, J. L., Nerem, R. S., and Tapley B. D.: 2000, 'Interannual Mean Sea Level Change and the Earth's Water Mass Budget', *Geophys. Res. Lett.* **27**, 3073–3076.

Chrgian, A. C.: 1978, 'Physics of the Atmosphere I' (in Russian), pp. 173 – 174, *Gidrometeoizdat*, Leningrad, 247 pp.

Chen, J. L., Wilson, C. R., Chambers, D. P., Nerem, R. S., and Tapley, D. B.: 1998, 'Seasonal Global Water Mass Budget and Mean Sea Level Variations', *Geophys. Res. Lett.* **25**, 3555–3558.

Gross, R. S.: 2000, 'The Excitation of the Chandler Wobble', *Geophys. Res. Lett.* **27**, 2329–2332.

Holland, W. R.: 1975, 'The Role of the Upper Ocean as a Boundary Layer in Models of the Oceanic General Circulation', in E. B Kraus (ed.), Modeling and Prediction of the Upper Layers of the Ocean. *Proc. NATO Advanced Study Institute, Urbino, Italy*.

Kouba, J., Beutler, G., and Rothacher, M.: 2000, 'IGS Combined and Contributed Earth Rotation Parameter Solutions', in S. Dick, D. D. McCarthy and B. Luzum (eds.), *Polar Motion Historical and Scientific Problems IAU Colloquium 178, The Astronomical Society of Pacific Series Conference Series*, Vol. 208, pp. 277–302.

Lemoine, F. G., Smith, D. E., Kunz, L., Smith, R., Pavlis, E. C., Pavlis, N. K., Klosko, S. M., Chinn, D. S., Torrence, M. H., Williamson, R. G., Cox, C. M., Rachlin, K. E., Wang, Y. M., Kenyon, S. C., Salman, R., Trimmer. R., Rapp, R. H., and Nerem, R. S.: 1997, 'The Development of the NASA GSFC and NIMA Joint Geopotential Model', *Proc. Int. Symp. Gravity, Geoid and Marine Geodesy, (GRAGEOMAR), Univ. of Tokyo, Japan, Sep. 30–Oct. 5, 1995*, Springer VLG, pp. 461–469.

McCarthy, D. D. (ed.): 1996, 'IERS Conventions (1996)', *IERS Technical Note*, 21, IERS Central Bureau at the Paris Observatory.

Ménard, Y., Jeanson, E., and Vincent, P.: 1994, 'Calibration of the TOPEX/POSEIDON altimeters at Lampedusa: Additional Results at Harvest', *J. Geophys. Res.,* **99**, 487–504.

Molodensky, M. S., Yeremeev, V. F., and Yurkina, M. I.: 1960, 'Methods for Study of the External Gravitational Field and Figure of the Earth, (in Russian)', *TRUDY TsNIIGAiK*, 131, Geodezizdat, Moscow. English transl.: Israel Program for Scientific Translations, 248 pp., Jerusalem 1962.

Ponte, R. M., Stammer, D., and Marshal, J.: 1998, 'Oceanic Signals in Observed Motions of the Earth Pole of Rotation', *Nature* **391**, 476–479.

Ponte, R. M. and Ali, A. H.: 2002, 'Rapid Ocean Signal in Polar Motion and Length of Day', *Geophys. Res. Lett.* **29** (15).

Rapp, R. H., Zhang, C., and Yi, Z.: 1996, 'Analysis of Dynamic Ocean Topography Using TOPEX Data and Orthonormal Functions', *Journ. Geophys. Res.– Oceanas*, **101** (C10), 485–494.

Salstein, D. A. and Rosen, R. D.: 1997, 'Global Momentum and Energy Signals from Reanalysis Systems'. Preprints, 7th Conf. on Climate Variations, *American Meteorological Society*, Boston, MA, pp. 344–348.